Electronic Supplementary Material

Electrocatalytic reduction of NO to NH_3 in ionic liquids by P-doped TiO_2 nanotubes

Shangcong Zhang[1,2], Qian Liu[3], Xinyue Tang[4], Zhiming Zhou[4], Tieyan Fan[4], Yingmin You (✉)[1,2], Qingcheng Zhang (✉)[4], Shusheng Zhang[5], Jun Luo[6], Xijun Liu (✉)[7]

1 College of Electrical and Electronic Engineering, Wenzhou University, Wenzhou 325035, China

2 Low Voltage Apparatus Technology Research Centre of Zhejiang, Wenzhou University, Zhejiang 325035, China

3 Institute for Advanced Study, Chengdu University, Chengdu 610106, Sichuan, China

4 College of Chemistry and Materials Engineering, Wenzhou University, Wenzhou 325035, China

5 College of Chemistry, Zhengzhou University, Zhengzhou 450000, China

6 Tianjin Key Lab for Photoelectric Materials & Devices, School of Materials Science and Engineering, Tianjin University of Technology, Tianjin 300384, China

7 MOE Key Laboratory of New Processing Technology for Non-Ferrous Metals and Materials, and Guangxi Key Laboratory of Processing for Non-Ferrous Metals and Featured Materials, School of Resource, Environments and Materials, Guangxi University, Nanning 530004, China

E-mails: yymfd@163.com (You Y); zhangqc@wzu.edu.cn (Zhang Q); xjliu@tjut.edu.cn (Liu X)

Figures and Table

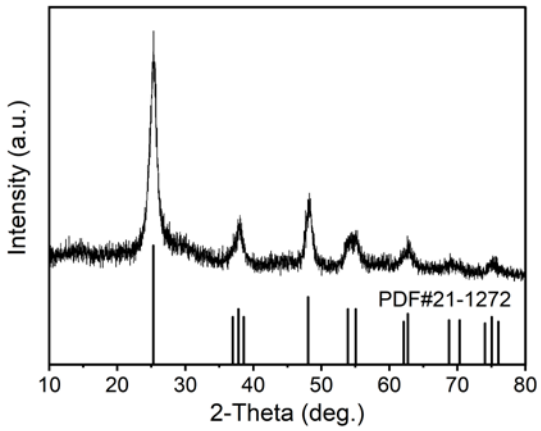

Figure S1. XRD pattern of the as-prepared TNTs. All the XRD peakscan be well assigned to the anatase phase TiO_2 (JCPDS No. 21-1272).

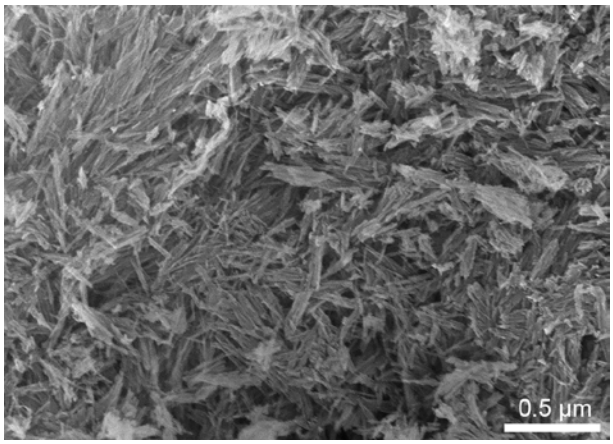

Figure S2. SEM image of the as-prepared TNTs.

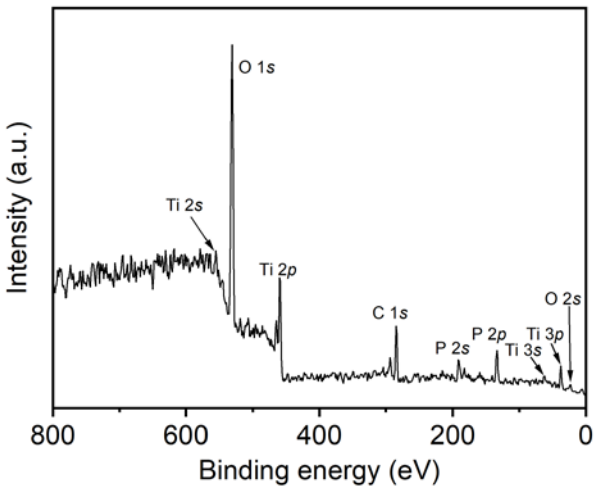

Figure S3. XPS spectrum of P-TNTs.

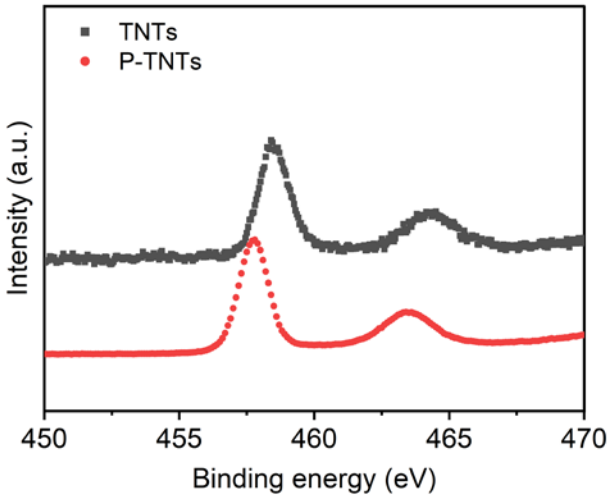

Figure S4. High-resolution of Ti 2*p* XPS spectrum of P-TNTs and TNTs.

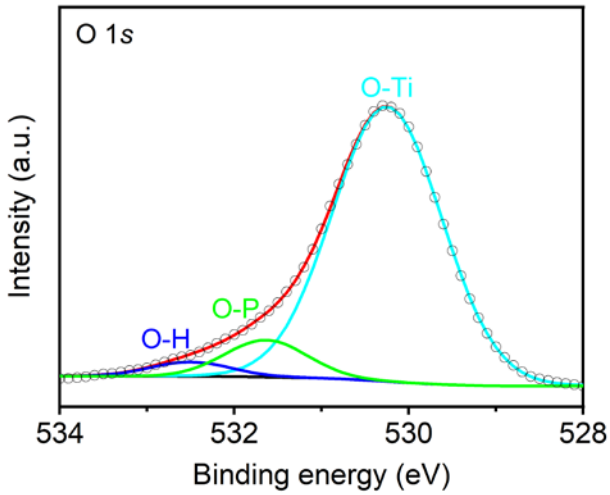

Figure S5. High-resolution of O 1*s* XPS spectrum of P-TNTs.

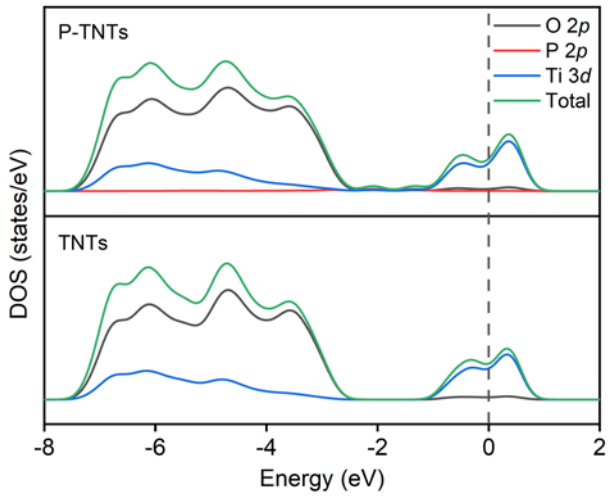

Figure S6. The calculated PDOS of P-TNTs and TNTs. It can be found that the new states between the valence band (VB) and conduction band (CB) mainly originate from the 2*p*

orbitals of P and O atom. The CB consists mainly of 3*d* orbitals of the Ti atom, and the VB is spanned mainly by the 2*p* orbitals of O atom and the 2*p* orbitals of P atom. Electrons excited from the mixing states of P 2*p* and O 2*p* to the CB decrease of the band gap of TiO_2,[34,35] which also favors the charge transfer during the electrolysis.

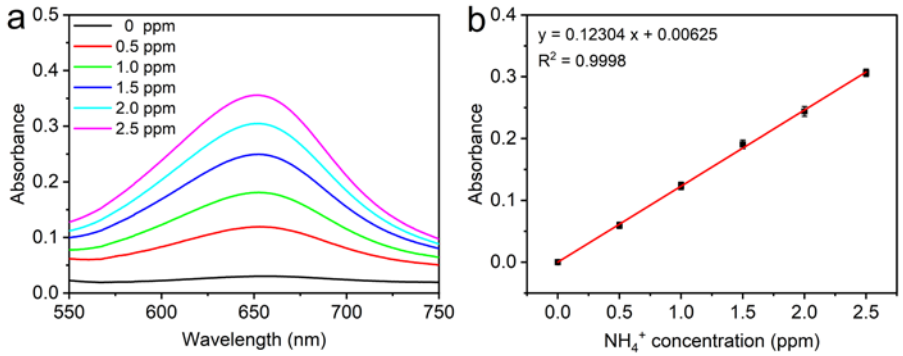

Figure S7. a The UV-Vis absorption spectra and **b** corresponding calibration curves for the colorimetric NH_3 assay using the indophenol blue method in electrolyte. The error bars correspond to the standard deviations of measurements over three separately independent experiments under the same conditions.

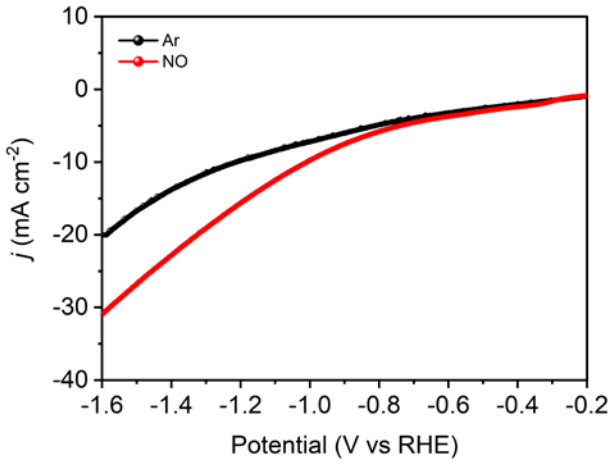

Figure S8. NORR polarization curves of P-TNTs in Ar- and NO-saturated IL electrolyte.

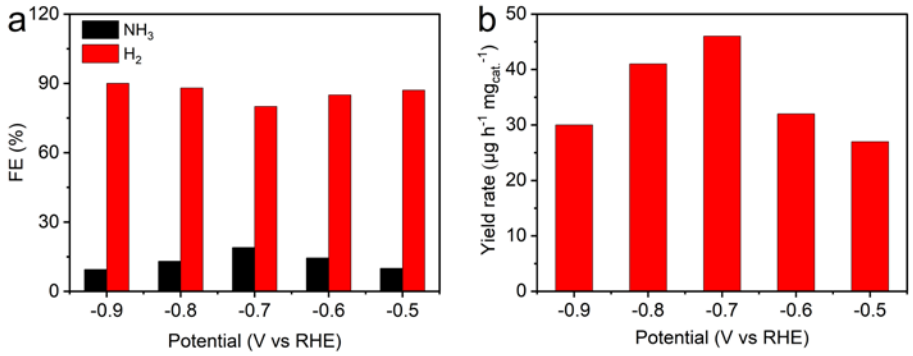

Figure S9. NORR performance of P-TNTs in aqueous electrolyte. (a) FE_{NH3} and FE_{H2} values at different working potentials. (b) NH_3 yield rates at different working potentials.

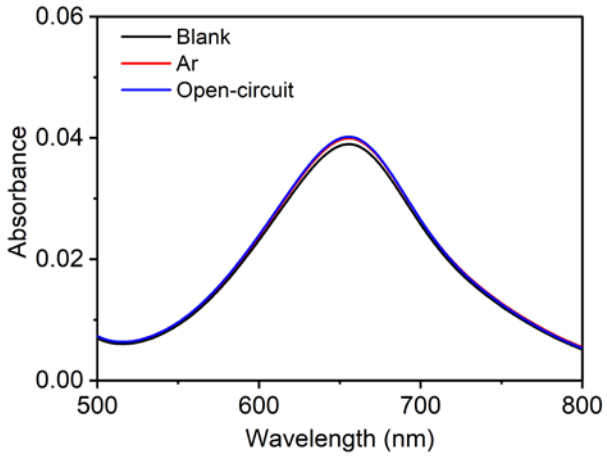

Figure S10. UV-Vis spectra of the electrolyte at different electrolysis conditions.

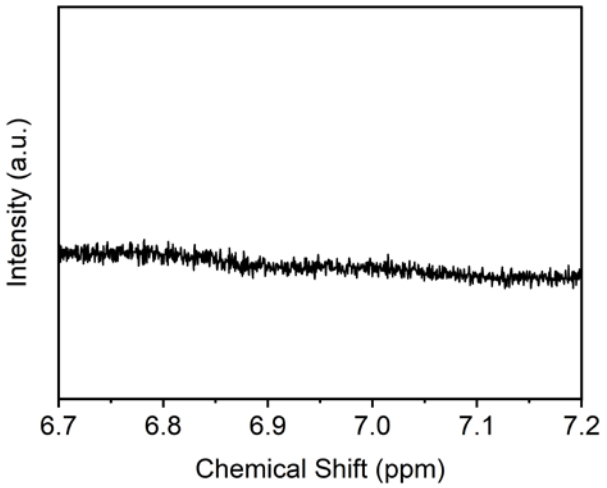

Figure S11. ^1H NMR spectrum of P-TNTs recorded in Ar-saturated IL electrolyte. No NH_3 can be detected.

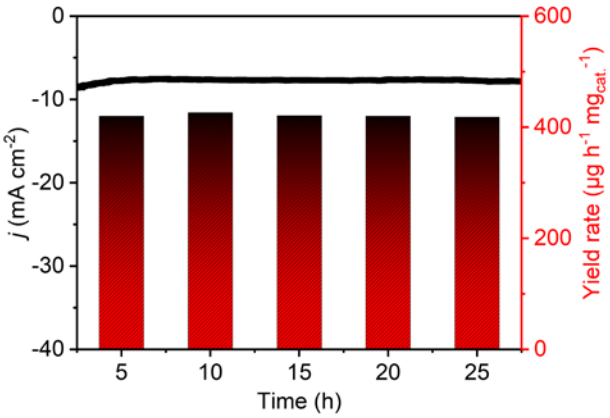

Figure S12. Constant potential electrolysis at -0.8 V vs RHE.

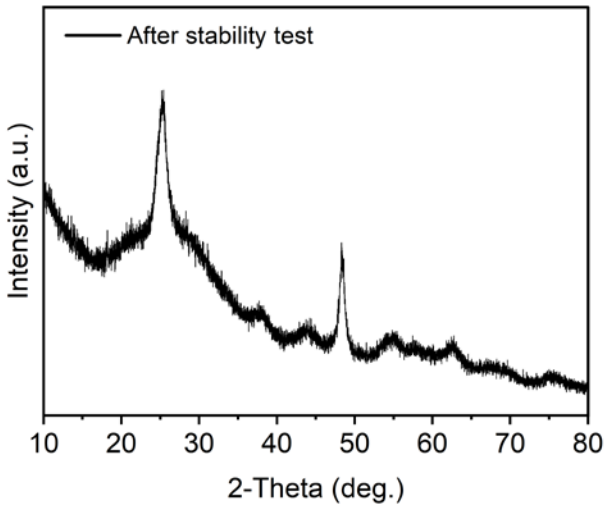

Figure S13. Additional XRD patterns of P-TNTs before and after stability test. Clearly, no additional peaks can be observed after the stability test.

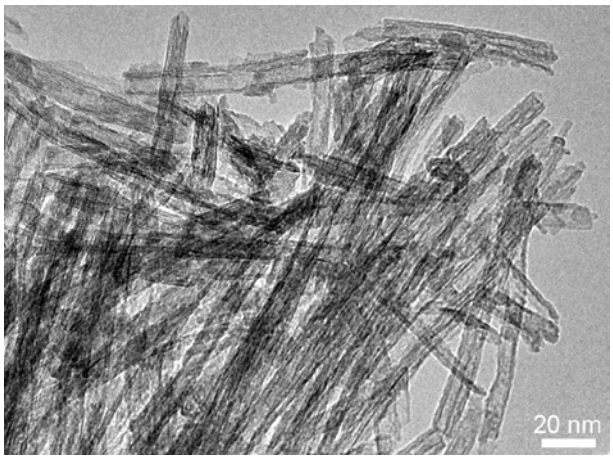

Figure S14. Additional TEM image of P-TNTs after stability test.

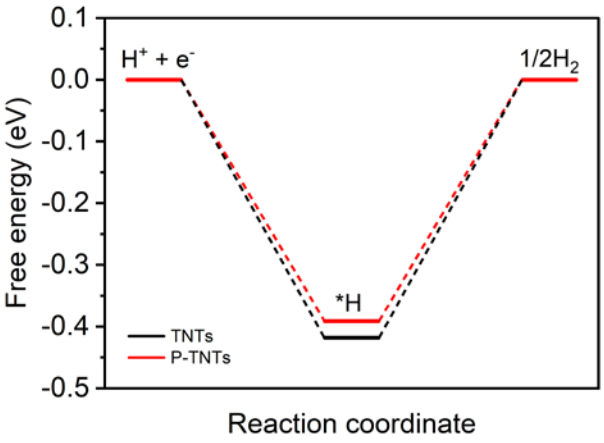

Figure S15. The energy change for the HER on P-TNTs and TNTs.

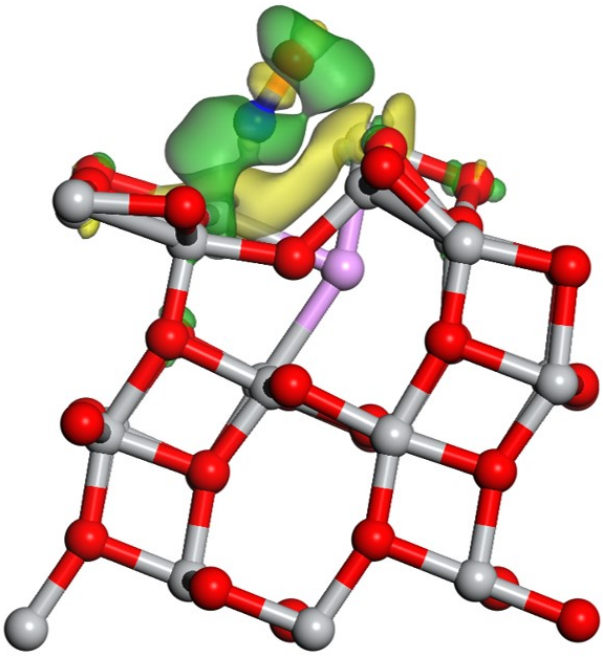

Figure S16. Atomic models with charge density difference plot of NO adsorption on P-TNTs. The green and yellow regions represent positive and negative charges, respectively.

Table S1. Electrocatalysis results from this work and those reported NRR and NORR results in the literature.

Catalyst	Electrolyte	NH_3 Yield Rate	FE (%)	Potential	Reference
Au/TiO_2 Au (1.542 wt%)	0.1 M HCl	21.4 μg $h^{-1}mg_{cat.}^{-1}$	8.11	–0.2 V vs RHE	*Adv. Mater.* 2017, 29, 1606550
a-Au/CeOx-RGO Au (1.31 wt%)	0.1 M HCl	8.3 μg h^{-1} $mg_{cat.}^{-1}$	10.10	–0.2 V vs RHE	*Adv. Mater.* 2017;29, 1700001
THH Au NRs	0.1 M KOH	1.648 μg h^{-1} cm^{-2}	4.02	–0.2 V vs RHE	*Adv. Mater.* 2017, 29, 1604799
PEBCD/C	0.5 M Li_2SO_4	1.58 μg $h^{-1}cm^{-2}$	2.85	–0.5 V vs RHE	*J. Am. Chem. Soc.* 2017, 139, 9771
$Pd_{0.2}Cu_{0.8}$/rGO	0.1 M KOH	2.8 μg h^{-1} $mg_{cat.}^{-1}$	~4.5	–0.2 V vs RHE	*Adv. Energy Mater.* 2018, 8, 1800124
N-doped porous carbon	0.05 M H_2SO_4	1.40 mmol g^{-1} h^{-1}	1.42	–0.9 V vs RHE	*ACS Catal.* 2018, 8, 1186
Au film	0.1 M KOH	3.84×10^{-12} mol cm^{-2} s^{-1}	<1	–0.5 V vs RHE	*J. Am. Chem. Soc.* 2018, 140, 1496
hollow Au nanocages	0.5 M $LiClO_4$	3.9 μg h^{-1} cm^{-2} (–0.5 vs RHE)	30.2	–0.4 vs RHE	*Nano Energy* 2018, 49, 316
RuPt/C	1 M KOH	1.04×10^{-8} g s^{-1} cm^{-2}	13.2	0.123 vs RHE	*Electrochem. Commun.* 2018, 90, 96
Boron-doped graphene	0.05 M H_2SO_4	9.8 μg h^{-1} cm^{-2}	10.8	–0.5 vs RHE	*Joule* 2018, 2, 1610

Amorphous $Bi_4V_2O_{11}/CeO_2$	0.1 M HCl	23.21 μg h^{-1} $mg_{cat.}^{-1}$	10.16	–0.2 vs RHE	*Angew Chem. Int. Ed.* 2018, 57, 6073
B_4C	0.1M HCl	26.57 μg h^{-1} $mg_{cat.}^{-1}$	15.95	–0.75 vs RHE	*Nat. Commun.* 2018, 9, 3485
Single Ru atoms	0.1 M HCl	120.9 μg h^{-1} $mg_{cat.}^{-1}$	29.6	–0.2 vs RHE	*Adv. Mater.* 2018, 0, 1803498.
SA-Mo/NPC	0.1 M KOH	34.0 ± 3.6 μg h^{-1} $mg_{cat.}^{-1}$ (34.0 ± 3.6 μg h^{-1} cm^{-2})	14.6 ± 1.6	–0.3 vs RHE	*Angew. Chem. Int. Ed. 2019, 58, 2321*
a-$B_{2.6}C$@TiO_2 (NORR)	0.2 M Na_2SO_4	3678.6 μg h^{-1} cm^{-2}	87.6	–0.9 vs RHE	*Angew. Chem. Int. Ed. 2022, e202202087*
MoS_2/GF (NORR)	0.1 M HCl + 0.5 mM Fe(II)SB	99.6 μmol h^{-1} cm^{-2} (281.1 μg h^{-1} $mg_{cat.}^{-1}$)	76.6	–0.7 vs RHE	*Angew. Chem. Int. Ed. 2021, 60, 25263*
Cu foam (NORR)	0.25 Li_2SO4	517.1 μmol h^{-1} cm^{-2}	93.5%	–0.9 vs RHE	*Angew. Chem. Int. Ed. 2020, 59, 9711*
$Ru_{0.05}Cu_{0.95}$ (NORR)	0.2 M Na_2SO_4	17.68 μmol h^{-1} cm^{-2}	64.9	–0.5 vs RHE	*Sci. China Chem. 2021, 64, 1493*
FeNC (NORR)	0.1 M $HClO_4$	~20.2 μmol h^{-1} cm^{-2}	~5.1	–0.2 vs RHE	*Nat. Commun. 2021, 12, 1856*
P-TNTs (NORR)	IL	425 μg h^{-1} $mg_{cat.}^{-1}$ (–0.9 vs RHE)	89	–0.8 vs RHE	*This work*